Science Journal of University of Zakho
DOI: https://doi.org/10.25271/sjuoz.2026.14.3.1625

**Original Article**

# INFLUENCE OF THERMAL TREATMENT ON CRYSTALLINITY, DEFECT STATE, STABILITY, AND PHOTONIC CHARACTERISTICS OF ZnO NANOPARTICLES

**Mohammed M. Hamadali[1,*], and Muhamad A. Hamad[1]**

[1]Department of Physics, College of Education, Salahaddin University-Erbil, Erbil, Kurdistan Region, Iraq.

[*]*Corresponding author, E-mail:*mohammed.m.hamadali@su.edu.krd (Tel: +964-7504931054)

Received
June 14, 2025

Accepted
January 14, 2026

Published
July 2, 2026

**ABSTRACT**

The sol-gel technique was successfully used to synthesize zinc oxide nanoparticles (ZnO NPs), using zinc acetate dihydrate as a precursor and sodium hydroxide as a precipitating agent to examine the influences of thermal treatment on the structural, morphological, and optical behaviour. Calcination was conducted at different temperatures ranging from 450 °C to 750 °C. The achieved Zinc oxide nanoparticles were analyzed using various characterizations, including field emission scanning electron microscopy (FESEM), X-ray diffraction (XRD), UV-visible spectroscopy, and zeta potential analysis. The outcomes showed that calcination significantly affects crystallinity, particle size, bandgap, and stability. The ideal temperature emerged to be 550 °C. X-ray diffraction validated the development of hexagonal wurtzite, demonstrating the highest crystallinity at 91.27%, the lowest crystallite size of 18.668 nm, the narrowest optical bandgap of 3.62 eV, and the best colloidal stability of -55.17 mV. These findings underscore the significance of heat control in tuning the properties of ZnO nanoparticles, rendering them appropriate for diverse applications in nanotechnology and optoelectronics.

**Keywords:** ZnO Nanoparticles, Sol-gel, Calcination temperature, Crystallinity, Stability.

## 1. INTRODUCTION

Nanotechnology is widely applied in the fields of chemistry, biology, physics, and materials science. In at least one dimension, it involves the creation, characterisation, and use of materials as well as the design of devices operating in the nanoscale range of one to one hundred nanometers (Kotousov *et al*., 2014). Their distinctive characteristics, especially their large surface-to-volume ratio, make them crucial components in technological development (S. M. Ismail & Ahmed, 2023). According to Moore's Law, from 1975 to 2011, integrated circuits have experienced a doubling in transistors and a reduction in size nearly every two years (Burg & Ausubel, 2021). This trend, called Moore's Law, has led to enhanced design precision, increased operating speed, and a demonstration of nanotechnology capabilities. As size diminishes, new chemical interactions and biological processes, such as targeted drugs bonding and delivery, occur at the nanoscale (Malik *et al*., 2023).

A particle of substance whose diameter ranges from one to a hundred nanometers is called a nanoparticle (Khan & Hossain, 2022). Their distinct physical and chemical properties, which are absent at the microscopic level, set them apart from bulk materials. The decrease in size implies that the desirable property can be easily obtained in nanostructures. Nearly all properties of matter change when it goes to the nanoscale (Altammar, 2023). Nanoparticles are categorized into six groups based on shape, size, and chemical composition. Carbon-based nanoparticles are optimal for electronic and energy applications owing to their electrical conductivity, mechanical strength, and flexibility (Fadaie *et al*., 2021). Metal nanoparticles such as gold and silver exhibit unique electrical and optical characteristics related to localized Surface Plasmon Resonance (SPR) (Alzoubi *et al*., 2023). Ceramic nanoparticles have thermal stability and chemical inertness, and are widely used in coatings, catalysis, and energy preservation technologies (Samantaray *et al*., 2024). Nanoparticles of lipids are used to deliver drugs, genes, and vaccines (Bolhassani, 2023).

Zinc oxide nanoparticles (ZnO NPs) have garnered significant interest in nanotechnology and nanoscience owing to their unique structural, optical, and electrical features (Sridar *et al*., 2018). ZnO nanoparticles demonstrate several characteristics such as non-toxicity (Nagar *et al*., 2022), being inexpensive and secure (Nandhini *et al*., 2024), biocompatibility, UV protection, antibacterial properties, high thermal conductivity, and can be synthesized easily (Bekele *et al*., 2021; Shafiee *et al*., 2021). These attributes make them highly suitable for various products, including solar cells, rubber, cosmetics, and medical and pharmaceutical items (Shafiee *et al*., 2021). ZnO NPs are the second most abundant metal oxide nanomaterial after iron, composed of zinc and oxygen. They are a white powder with a wide direct bandgap about 3.37 eV and high exciton binding energy, approximately 60 meV (Mahajan *et al*., 2025). Zinc oxide exhibits strong ultraviolet emission, chemical stability, and a variety of morphologies, rendering it a valuable material for diverse utilizations such as optoelectronics, photo catalysis, gas sensing, and bio sensing (Gopinath, 2020; Tripathy & Kim, 2018). It serves as a glass modifier, lowering the melting point, boosting glass formation capability, and improving optical and structural properties due to an appropriate band gap and significant exciton binding energy at room temperature (Mohamed & Mawlud, 2023). Various physical, chemical, and biological approaches are employed extensively in the synthesis of nanoparticles. In contrast, the fabrication of nanoparticles via physical and chemical processes, which produce various sizes and shapes, requires stable agents as they are often unstable (Azeez Abdullah Barzinjy & Azeez, 2020). These methods offer particular, identifiable characteristics. While physical and chemical processes have been considered

Access this article online

DOI:https://doi.org/10.25271/sjuoz.2026.14.3.1625

Printed ISSN 2663-628X;
Electronic ISSN 2663-6298

**Science Journal of University of Zakho**
**Vol. 14, No. 03, pp. 432-439, July -2026**

better, especially for producing homogenous stable nanostructures, they fail to achieve the objective of ensuring long-term sustainability (Ahmed *et al*., 2016). Many techniques, including sol-gel, precipitation, solvothermal, and microwave-assisted approaches, have been employed to synthesize ZnO nanoparticles (Sugihartono *et al*., 2019). Among the approaches, the sol-gel approach is one of the most attractive that has been considered the most practical method because of the lower cost of equipment compared to other methods, and it is easy to gain nanoparticles with good homogeneity (Mahato *et al*., 2023).

An essential stage in preparing ZnO nanoparticles is thermal treatment, specifically calcination. This process requires heating the nanoparticles at a temperature that remains less than the melting point of ZnO nanoparticles and under high pressure to eliminate impurities, regulate agglomeration, and control size. The temperature and duration of calcination were crucial in improving the activity of ZnO nanoparticles as a photo catalyst (Supin *et al*., 2023). Consequently, enhancements in crystallinity, grain growth, and the reduction of lattice strain are noted with increased calcination temperatures. Still, these may also be associated with changes in defect density and surface area, which directly influence the optical properties (V. Sharma *et al*., 2023), electrical conductivity (ElFaham *et al*., 2021), morphology (A. M. Ismail *et al*., 2019), and crystallinity (Usman *et al*., 2022).

While there has been significant investigation into ZnO nanomaterials, a thorough understanding of how various thermal treatments influence the interactions between crystallinity, defect states, and optical properties, particularly in sol-gel synthesized nanoparticles, has not yet been fully established. Numerous studies have concentrated on individual factors, like crystallite size or luminescence, while excluding their collective impact on stability and functional performance under varying thermal conditions. This study addresses the problem by seriously investigating the effect of thermal treatment on ZnO nanoparticles produced via the sol-gel method. The goals are to examine the development of crystallinity and defect structures across different calcination temperatures, evaluate the stability of nanoparticles in terms of their structural stability, and analyze the changes in optical behavior induced by temperature, particularly focusing on the optical band gap.

## 2. MATERIALS AND METHODS

Zinc acetate dihydrate [Zn $(CH_3COO)_2 \cdot 2H_2O$] with a molecular weight of 219.49 g/mol and 99% purity was employed as a metallic precursor, while sodium hydroxide (NaOH), with a molecular weight of approximately 40 g/mol, was utilized without additional purification; both were procured from Scharlau is based in Spain. Absolute ethanol ($C_2H_5OH$, 96% purity) from Sigma Aldrich, and deionized water with around 98% purity was elected as solvents.

### Synthesis of ZnO NPs:

Zinc oxide nanoparticles were synthesized utilizing the sol-gel method, as shown in Figure 1. An amount of 5.47 g of zinc acetate dihydrate was dissolved in 100 mL of ethanol to prepare a 0.25 M solution, and the mixture was stirred for 15 minutes using a magnetic stirrer to achieve complete dissolution. A sodium hydroxide solution was prepared by dissolving 1.2 g of sodium hydroxide (NaOH) in 20 mL of deionized water and stirring for 10 minutes. The solution was gradually titrated into the zinc acetate solution, and the pH was adjusted to 9 while continuously stirring at 60 °C to ensure full hydrolysis, resulting in a white paste after 2 hours. The solution was allowed to settle for 24 hours at room temperature, boosting condensation processes. The suspension was centrifuged at 3500 rpm to obtain a homogeneous ZnO nanoparticle precipitate.

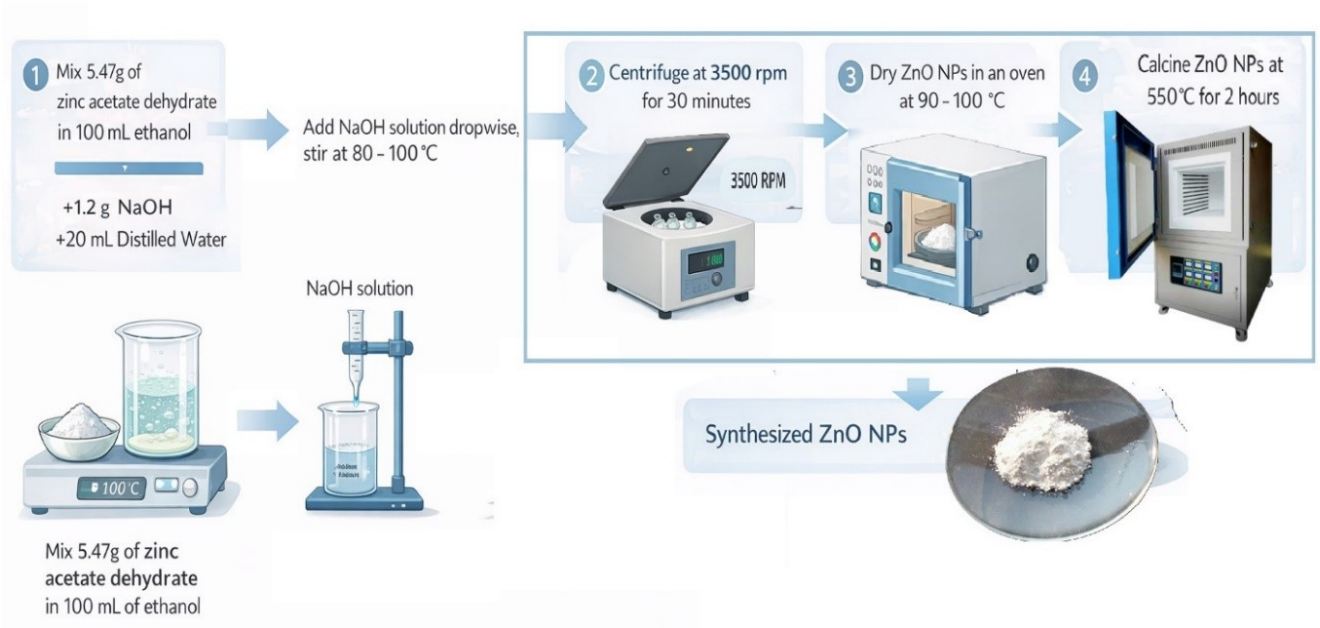


**Figure 1:** Systematic illustration of preparing ZnO NPs by the Sol-gel method using Zinc acetate dehydrate.

Subsequently, the solution was transferred to a drying oven at 100°C for 2 hours to remove the solvent and water, producing approximately 2 g of white ZnO Nano powder. Then, one sample was kept un-calcined (room-temperature dried) as a control. Meanwhile, another seven samples were calcined using a high-temperature Muffle Furnace (BIOBASE MC2.5- 12 Lab, 1200°C) for 2 hours at various temperatures of 450, 500, 550, 600, 650, 700, and 750°C, respectively. After calcination, colour of the produced ZnO NPs regained a white or pale-yellow color, as shown in Figure 2.

### Characterization Techniques:

A structural investigation was conducted utilizing the XRD technique with a Bruker D8 Discover diffractometer to identify the crystallite size and degree of crystallinity of ZnO nanoparticles. The source of X-rays was Cu Kα radiation (λ = 0.153 nm). The scanning rate was 0.2 degrees per second, recorded in the 2θ range from 10° to 80°. The optical absorption spectra of the ZnO nanoparticles and their optical energy gap were measured at room temperature using a double-beam UV-Vis spectrophotometer (Shimadzu 1301PC)

within the wavelength range of 300 to 800 nm to confirm the synthesis of ZnO nanoparticles. Morphology and particle dispersion can be assessed using a Field Emission Scanning Electron Microscope (FESEM) at an accelerating voltage of roughly 15 kV (MIRA3 TECSAN). The stability of the material was assessed by its zeta potential spectrum utilizing the HORIBA Scientific SZ-100 model.

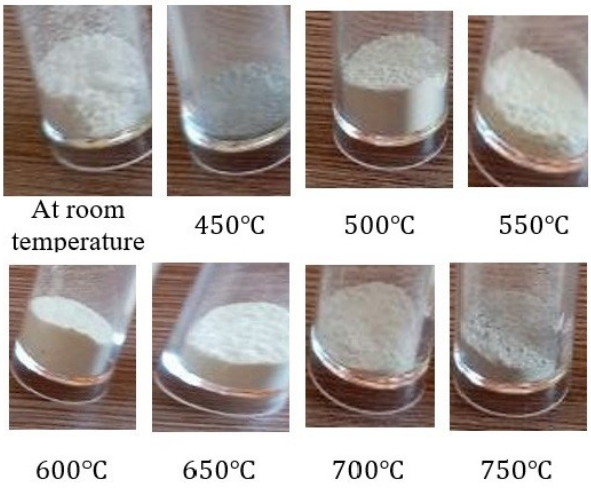


**Figure 2:** Synthesized ZnO Nps by the Sol-gel method before calcination and at various temperatures from 450 °C to 750 °C.

## 3. RESULTS AND DISCUSSION

### UV-Visible Analysis:

UV-Visible Spectroscopy is the most widely used technique for studying the optical characteristics of ZnO NPs. Following synthesis, the calcination procedure affects the optical properties of ZnO NPs and aids in agglomeration control (Alibe *et al*., 2017). Figure 3 describes the UV-Visible absorbance spectrum of ZnO NPs before calcination and at various calcination temperatures ranging from 450 to 750 °C. Significant variations in photonic behaviour are revealed, primarily observed in the position and intensity of the absorbance edges. It is observed that, at room temperature, ZnO NPs exhibit an absorption peak around 372.38 nm, which shifts towards higher wavelengths (red shift) upon rising temperature, reaching approximately 381.38 nm at around 550 oC, which indicates a reduction in optical energy gap. This is attributed to enhanced crystallinity, particle size growth, and reduction of surface defects (Kaur *et al*., 2025). As thermal treatment progresses, the ZnO Nanocrystals grow in size due to grain coalescence and reduce the quantum confinement effect. This effect leads to a narrowing band gap, as previously reported by Şimşek *et al*., (2022) and Azeez A Barzinjy *et al*., (2020). They observed that higher calcination temperatures improve structural order and crystallinity in ZnO Nps, directly affecting optical absorption behaviour. However, the shift towards smaller wavelengths exhibits a blue shift after 550 °C, which indicates an increase in the optical band gap. which is attributed to the reduction of defect states such as oxygen vacancies and interstitial zinc, which are responsible for sub-bandgap transitions and lead to a wider bandgap (Kayaci *et al*., 2014). It can cause agglomeration or saturation in grain growth, and altering the crystalline structure as previously reported by R. Sharma *et al*. (2023).

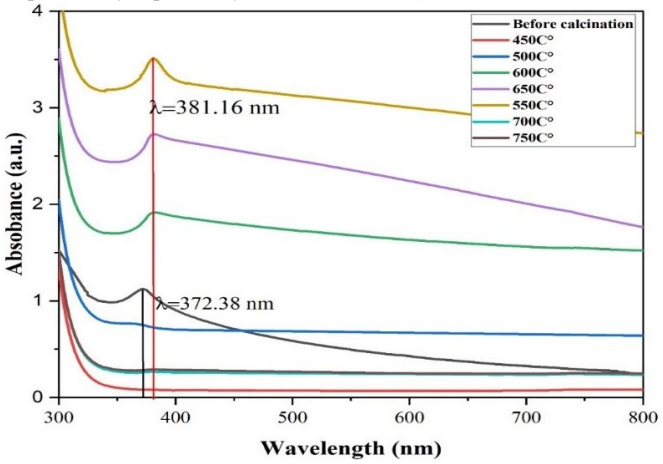


**Figure 3:** UV-Visible spectra of ZnO NPs before and after calcination at various temperatures.

The band gap energy ($E_g$) of ZnO nanoparticles was evaluated by fitting the optical reflection data using the Tauc equation. This analysis was carried out to investigate the impact of thermal treatment on the optical properties of the nanoparticles.

$$\alpha h\nu = A(h\nu - E_g)^n \quad (1)$$

Where $\alpha$ is the optical absorbance coefficient, h$\nu$ indicates photon energy, $A$ is the proportionality Constant, and $n$ represents the type of optical transitions, 1/2 for direct and 2 for indirect transitions (Parajuli *et al*., 2023). The amount of band gap is calculated through the extrapolation of the rectilinear part of the plot, as observed in Figure 4. The band gap decreases from 3.91 eV to 3.62 eV when the temperature increases from 450 to 550 °C. This consequence does not conflict with the effects of quantum confinement. Furthermore, after 550 °C, as observed at the range between 600 and 750 °C, the energy gap changes from 3.75 eV to 3.98 eV with increasing temperature, which distorts the band structure, shifting the band gap undesirably as previously reported by Pal Singh *et al*. (2016).

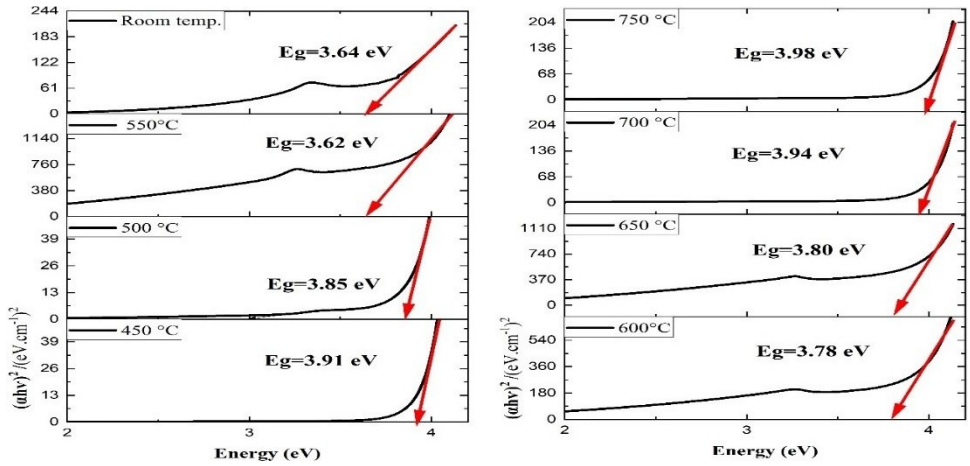


**Figure 4:** UV-Visible spectra of ZnO NPs before and after calcination at various temperatures.

As observed, 550 °C appears to be an optimal temperature at which the absorption edge becomes sharper compared to lower temperatures (450 –500 °C), suggesting a reduction in structural defects and residual impurities. Moreover, the optical band gap at 550 °C is measured to be 3.62 eV, which is closer to the expected bulk ZnO value of about 3.3 eV than the values achieved at lower or higher calcination temperatures. This indicates that 550 °C provides a balance between enhanced crystallinity and minimal agglomeration, and therefore enhances the optical properties of ZnO nanoparticles.

## XRD Analysis:

The structural properties of the synthesized ZnO Nps before and after increasing temperature from 450 to 750 °C were investigated using XRD. Figure 5 describes how the patterns are different in intensity and the crystallinity of the ZnO NPs according to calcination temperatures. This confirms that ZnO NPs is crystalized, as a hexagonal wurtzite structure according to detected (hkl) planes including the (100), (002), (101), (102), (110), (103), and (200), which appear from the XRD patterns, were indexed from the standard database (JCPDS card no. 03-065-3411). This result was also reported by Zubair *et al*. (2023) and Kumar *et al*. (2024).

According to the findings, X-ray diffraction intensity rose with calcination temperature until it reaches 550 oC. However, in the range of 650-750 oC, it decreased, most likely as a result of crystallinity changes. The average crystallite size of ZnO NPs has been estimated by Debye-Scherrer's equation:

$$D = \frac{K\lambda}{\beta \cos(\theta)} \tag{2}$$

Where $labmda$ indicates the wavelength of the X-ray source is approximately (1.54Å), K is scherrer constant which is 0.9, referred to as a shape factor, $\beta$ is the full width at half maximum (FWHM) of each peak, $\theta$ is the peak position, and $D$ is the crystallite size (Holzwarth & Gibson, 2011).

According to the Debye-Scherrer equation, the average crystallite size for ZnO NPs was 18.668 nm, which confirmed the nano-sized ZnO nanoparticles at 550 ℃ (Table 1).

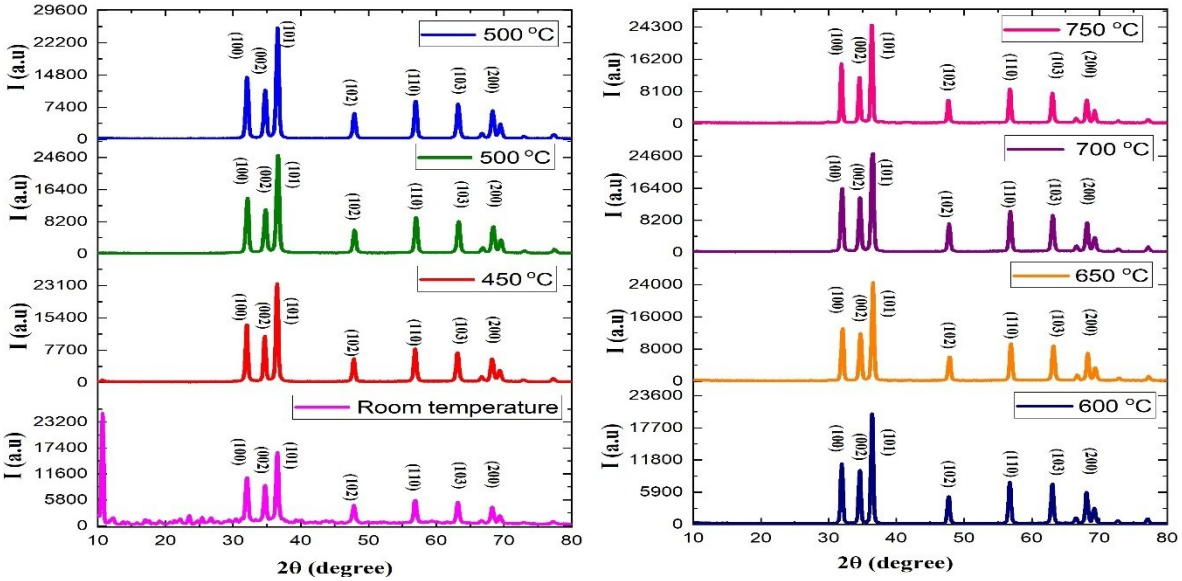


**Figure 5:** XRD Patterns of ZnO NPs before and after calcination at various temperatures.

Furthermore, investigations show that the average crystal sizes are between (18.668 - 23.65 nm) for the temperature increase between (450-750 °C), and it was observed that the smallest crystallite size of ZnO NPs was obtained at 550 °C. XRD analysis shows the existence of even tinier nanoparticles than the FESEM micrograph. The larger ZnO nanoparticles are due to agglomeration of smaller nanoparticles indicated by X-ray diffraction.

## FESEM Analysis:

The impact of calcination at different temperatures on the shape and average size distribution of ZnO nanoparticles was analysed using Field Emission Scanning Electron Microscopy (FESEM), as illustrated in Figure 6. It is evident that the majority of ZnO nanoparticles, regardless of temperature, are predominately nanoscale and exhibit a hexagonal morphology that seems spherical. FESEM indicates that as the temperature rises from 450 to 500 ℃, the particles appear loosely packed with irregular shapes and relatively small average sizes. However, during the temperature range of 600 to 750 ℃, the average size distribution is around (76.24 nm to 84.7 nm), indicating significant agglomeration, incomplete crystallization, and limited particle growth. As shown in Figure 6(h), the nanoparticles immediately before calcination show large, undefined agglomeration and are affected by various environmental factors such as humidity, oxygen exposure, pH, and ionic strength, which can increase average particle size and significantly impact the stability of nanoparticles and their aggregations (Bian *et al*., 2011).

Consequently, during the nanoparticle formation, the nanoparticles adhere to one another and spontaneously form asymmetrical clusters (Loza *et al*., 2019). The smallest particle size is in the range 550 ℃. The average particle size reduces to (48.32 ±17.3 nm). As shown in Figure 6(c), particles become more uniform and spherical, which suggests optimal crystallinity and minimal agglomeration. The crystallinity rate of fabricated ZnO Nanoparticles is calculated through the following formula (Sa *et al*., 2017):

$$\text{Crystallinity}(\%) = \frac{\text{Area of crystalline peaks}}{\text{Total area (Crystalline+Amorphous)}} \times 100\% \tag{3}$$

**Table 1:** Particle sizes of ZnO nanoparticles before and after calcined at various temperatures, calculated using Debye–Scherrer's equation.

| Calcination Temperature (°C) | No. of Peaks | Plane (hkl) | Pos. [°2Th.] | FWHM [°2Th.] | Size (nm) | Average Size (nm) |
|---|---|---|---|---|---|---|
| **Before calcination** | 1 | (100) | 32.0659 | 0.4428 | 18.6671 | **22.49** |
| | 2 | (002) | 34.6714 | 0.3936 | 21.1441 | |
| | 3 | (101) | 36.4792 | 0.3444 | 24.2873 | |
| **450** | 1 | (100) | 32.0844 | 0.492 | 16.8012 | **19.46** |
| | 2 | (002) | 34.8628 | 0.3936 | 21.1552 | |
| | 3 | (101) | 36.6286 | 0.492 | 17.0085 | |
| **500** | 1 | (100) | 32.0178 | 0.3444 | 23.9977 | **22.68** |
| | 2 | (002) | 34.6308 | 0.3444 | 24.162 | |
| | 3 | (101) | 36.4317 | 0.3936 | 21.2485 | |
| **550** | 1 | (100) | 32.0277 | 0.3444 | 23.9983 | **18.668** |
| | 2 | (002) | 34.7703 | 0.492 | 16.9199 | |
| | 3 | (101) | 36.5771 | 0.492 | 17.0059 | |
| **600** | 1 | (100) | 31.9557 | 0.3444 | 23.994 | **23.653** |
| | 2 | (002) | 34.5643 | 0.3444 | 24.1577 | |
| | 3 | (101) | 36.371 | 0.3936 | 21.2448 | |
| **650** | 1 | (100) | 32.034 | 0.4428 | 23.994 | **23.658** |
| | 2 | (002) | 34.8039 | 0.3936 | 24.1577 | |
| | 3 | (101) | 36.6027 | 0.3444 | 21.2448 | |
| **700** | 1 | (100) | 32.0208 | 0.3444 | 23.9979 | **22.03** |
| | 2 | (002) | 34.6242 | 0.3936 | 21.1414 | |
| | 3 | (101) | 36.5678 | 0.3936 | 21.2568 | |
| **750** | 1 | (100) | 32.0136 | 0.3936 | 20.9978 | **20.931** |
| | 2 | (002) | 34.6288 | 0.4428 | 18.7926 | |
| | 3 | (101) | 36.4235 | 0.4428 | 18.8871 | |

And the crystallinity proportion ranges from 83.84 % to 91.27 % as the temperature rises from 450 ℃ to 550 ℃. After 550 ℃, especially from 600 ℃ to 750 ℃, the values decreased from 78.196 % to 75 %. The optical band gap and crystallinity are not simply inversely proportional. Instead, it is a complicated one that is affected by several variables, including impurities, which may cause the bandgap to decrease even in highly crystalline materials (Roy *et al*., 2024). These observations confirm that thermal treatment plays a crucial role in tuning particle size and morphology, with 550 ℃ emerging as a suitable temperature for synthesizing well-defined nanosized ZnO NPs. This result attributed that 550 ℃ is a critical temperature to reduce agglomeration and achieve a higher degree of crystallinity of sol-gel synthesized ZnO NPs (Table 2). There is a noticeable discrepancy between the XRD-determined crystallite size (18–24 nm) and the FESEM-measured particle size (48–85 nm). XRD estimates the size of individual crystalline domains, while FESEM visualizes entire particles, which may consist of multiple crystallites that have clustered together. During calcination, nanoparticles naturally undergo agglomeration due to high surface energy and attractive inter-particle forces, causing several crystallites to merge into larger secondary particles. Thus, the larger FESEM particle size reflects agglomerated assemblies of primary crystallites detected by XRD.

## FESEM Analysis:

The thermal treatment at different calcination temperatures can profoundly influence the surface charge and colloidal stability of ZnO nanoparticles, as analysed using zeta potential measurements. Zeta potential for highly stable particles values is generally greater than ±30 mV, which can stabilize a process that uses electrostatic repulsion. Nevertheless, positively charged particles are more effective in augmenting the electrical contact with the negatively charged visual surface (Onugwu *et al*., 2023). Figure 7 illustrates that the zeta potential is comparatively low at -2.73 mV just before calcination. This signifies insufficient stability due to inadequate surface charge for avoiding agglomeration at a temperature of 550 °C, the zeta

**Table 2:** Particle sizes of ZnO nanoparticles before and after calcined at various temperatures, calculated using Debye–Scherrer's equation.

| Temperature (°C) | Crystallite size (nm) (XRD) | Crystallinity (%) | Average Particle size (nm) FESEM |
|---|---|---|---|
| **Before Calcination (at room temperature)** | 22.49 | 83.846 | 61.31 ± 23.11 |
| **450** | 19.468 | 86.156 | 60.434 ± 10.68 |
| **500** | 22.685 | 86.16 | 52.26 ± 17.98 |
| **550** | 18.665 | 91.27 | 48.32 ± 17.3 |
| **600** | 23.658 | 78.196 | 84.31 ± 27.16 |
| **650** | 23.72 | 80.206 | 76.24 ± 37.99 |
| **700** | 22.031 | 82.517 | 71.66 ± 22.82 |
| **750** | 20.938 | 75.0057 | 84.70 ± 23.51 |

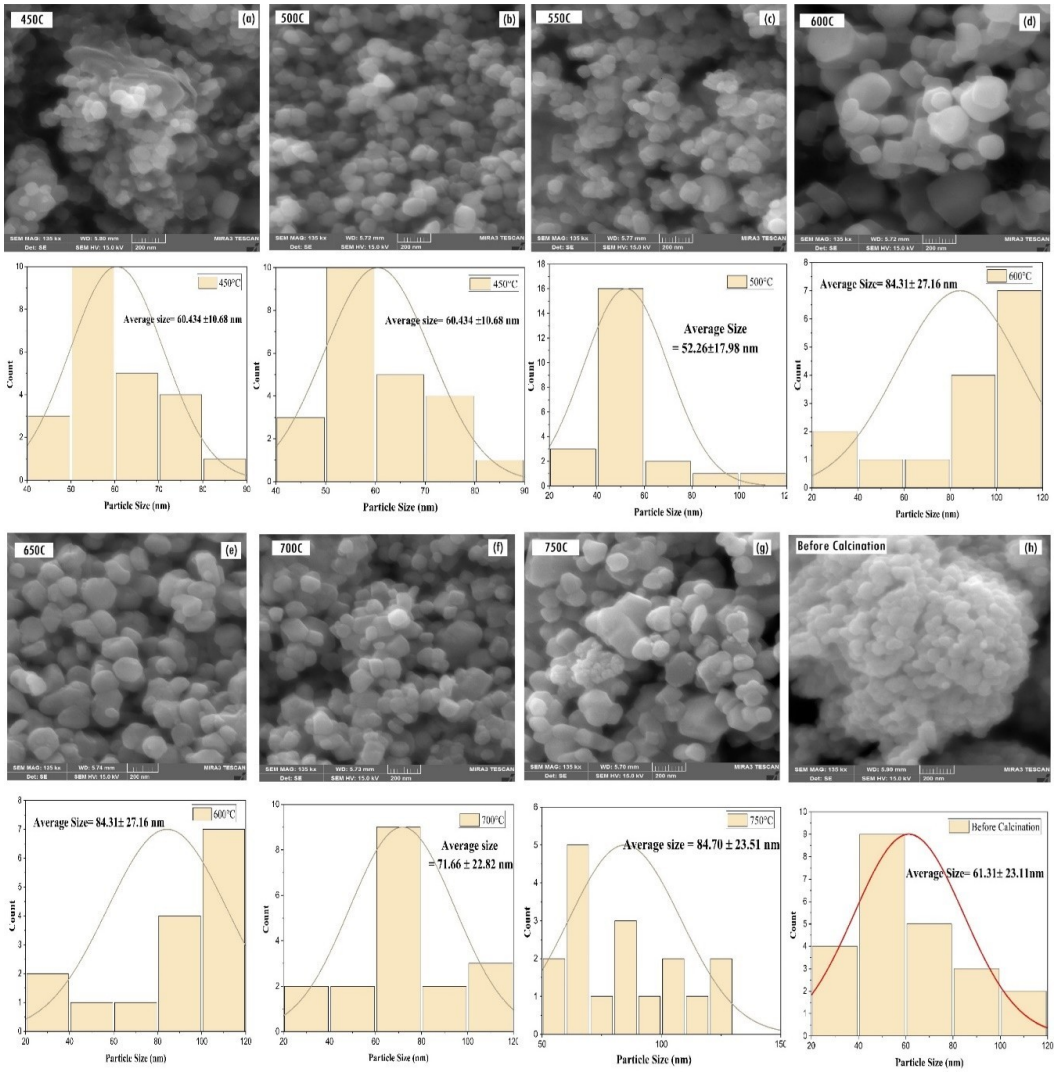


**Figure 6:** FESEM micrographs of ZnO NPs synthesized via the sol-gel method and calcined at different temperatures. Improved particle uniformity and reduced agglomeration are observed at 550 °C, while growth and clustering increase above this temperature.

potential reaches a notably negative value of -55.17 mV, indicating an increase in surface charge and electrostatic repulsion, enhancing dispersion stability.

The enhancement has been attributed to eliminating surface-adsorbed organic molecules and increasing crystallinity to 91.27 %, which reveals a greater amount of hydroxyl groups or lattice oxygen on the nanoparticle surface (Owuna, 2020). Increasing the calcination temperature to 750 °C provides a zeta potential of -27.26 mV, indicating less stability caused by grain growth at greater temperatures, which decreases surface area and active sites (Chang *et al*., 2024). Therefore, calcinations show that 550 °C is optimum for maintaining high stability in sol-gel-synthesized ZnO nanoparticles, which can significantly enhance nanoparticle dispersion.

## 4. CONCLUSION

In this work, ZnO NPs were synthesized effectively through the sol-gel method utilizing Zinc acetate dihydrate. And the impact of thermal treatment on their structural, morphological, crystallinity, and optical properties was successfully evaluated. Different characterization techniques using XRD, FESEM, zeta potential analysis, and UV–Visible spectroscopy revealed that thermal treatment plays a crucial role in governing crystallinity, particle size distribution, optical band gap, and colloidal stability. The study identifies 550 °C as an optimal calcination temperature at (pH ≈ 9), where ZnO nanoparticles exhibit improved morphological uniformity with the lowest agglomeration, highest degree of crystallinity, a narrowed optical band gap, presenting significant enhanced colloidal stability indicated by a negative zeta potential. In conclusion, these findings demonstrate that precise thermal control enables a good balance among structural, optical, and stability-related properties rather than improving a single parameter in isolation, which renders the nanoparticles suitable for increasing their applicability for optoelectronic applications.

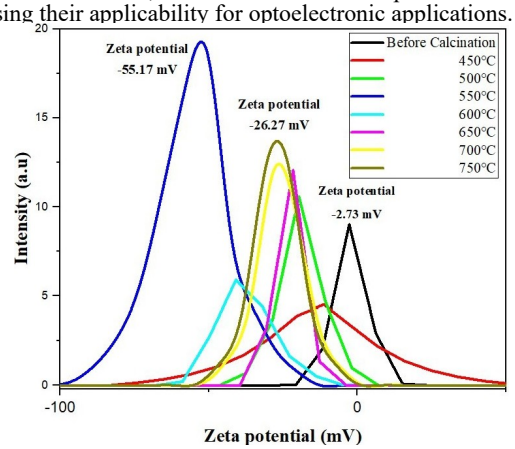


**Figure 7:** Zeta potential of synthesized ZnO NPs before calcination and calcined at different temperatures from 450 °C to 750 °C.

**Acknowledgment:**

The author expresses deep gratitude for the financial support from the Ministry of Higher Education and Scientific Research and the University of Salahaddin-Erbil, under the auspices of the Ministry of Higher Education, KRG.

**Ethical Statment:**

This article does not include any studies involving human participants or animals performed by the authors; therefore, ethical approval was not required.

**Conflict of Interests:**

We confirm no conflicts of interest or relationships with any other party.

**Funding:**

This study was financially supported by Salahaddin University- Erbil.

**Author Contributions:**

M.M.H. implemented data collection, conceptualized the study, analysed the data, and wrote the manuscript. While M.A.H. involved by reviewing and supervision of this present work. we further declare that all authors contributed, checked and approved the manuscript.

## 5. REFERENCES

Ahmed, S., Saifullah, Ahmad, M., Swami, B. L., & Ikram, S. (2016). Green synthesis of silver nanoparticles using Azadirachta indica aqueous leaf extract. *Journal of Radiation Research and Applied Sciences*, 9(1), 1–7. DOI:https://doi.org/10.1016/j.jrras.2015.06.006

Alibe, I. M., Matori, A. K., Saion, E., Ali, A. M., & Zaid, M. H. M. (2017). The influence of calcination temperature on structural and optical properties of ZnO nanoparticles via simple polymer synthesis route. *Science of Sintering*, 49(3), 263–275. DOI:https://doi.org/10.2298/SOS1703263A

Altammar, K. A. (2023). A review on nanoparticles: characteristics, synthesis, applications, and challenges. *Front Microbiol*, 14, 1155622. DOI:https://doi.org/10.3389/fmicb.2023.1155622

Alzoubi, F., Ahmad, A. A., Aljarrah, I. A., Migdadi, A., & Al-Bataineh, Q. M. (2023). Localize surface plasmon resonance of silver nanoparticles using Mie theory. *Journal of Materials Science: Materials in Electronics*, 34(32), 2128. DOI:https://doi.org/10.1007/s10854-023-11304-x

Barzinjy, A. A., & Azeez, H. H. (2020). Green synthesis and characterization of zinc oxide nanoparticles using Eucalyptus globulus Labill. leaf extract and zinc nitrate hexahydrate salt. *SN Applied Sciences*, 2(5), 991. DOI:https://doi.org/10.1007/s42452-020-2813-1

Barzinjy, A. A., Hamad, S. M., Abdulrahman, A. F., Biro, S. J., & Ghafor, A. A. (2020). Biosynthesis, characterization and mechanism of formation of ZnO nanoparticles using Petroselinum crispum leaf extract. *Current Organic Synthesis*, 17(7), 558–566. DOI:https://doi.org/10.2174/1570179417666200628140547

Bekele, B., Jule, L., & Saka, A. (2021). The effects of annealing temperature on size, shape, structure and optical properties of synthesized zinc oxide nanoparticles by sol-gel methods. *Digest Journal of Nanomaterials Biostructures*, 16(2), 471–478. DOI:http://dx.doi.org/10.15251/DJNB.2021.162.471

Bian, S.-W., Mudunkotuwa, I., Rupasinghe, T., & Grassian, V. (2011). Aggregation and Dissolution of 4 nm ZnO Nanoparticles in Aqueous Environments: Influence of pH, Ionic Strength, Size, and Adsorption of Humic Acid. *Langmuir : the ACS journal of surfaces and colloids*, 27, 6059–6068. DOI:http://dx.doi.org/10.1021/la200570n

Bolhassani, A. (2023). Lipid-based delivery systems in development of genetic and subunit vaccines. *Molecular Biotechnology*, 65(5), 669–698. DOI:https://doi.org/10.1007/s12033-022-00624-8

Burg, D., & Ausubel, J. H. (2021). Moore's Law revisited through Intel chip density. *PloS one*, 16(8), e0256245. DOI:https://doi.org/10.1371/journal.pone.0256245

Chang, J. S., Saint, C. P., Chow, C. W., Bahnemann, D. W., & Chong, M. N. (2024). Recent innovations in engineering Zinc Oxide (ZnO) nanostructures for water and wastewater treatment: Pushing the boundaries of multifunctional photocatalytic and advanced biotechnological applications. *International Materials Reviews*, 69(7–8), 337–379. DOI:https://doi.org/10.1177/09506608241280421

ElFaham, M. M., Mostafa, A. M., & Mwafy, E. A. (2021). The effect of reaction temperature on structural, optical and electrical properties of tunable ZnO nanoparticles synthesized by hydrothermal method. *Journal of Physics and Chemistry of Solids*, 154, 110089. DOI:https://doi.org/10.1016/j.jpcs.2021.110089

Fadaie, N., Sheikhi, M., Mohammadi, T., Tofighy, M. A., Rajabzadeh, S., & Sahebi, S. (2021). Novel Plasma Functionalized Graphene Nanoplatelets (GNPs) incorporated in forward osmosis substrate with improved performance and tensile strength. *Journal of Environmental Chemical Engineering*, 9(4), 105708. DOI:https://doi.org/10.1016/j.jece.2021.105708

Gopinath, S. C. (2020). Nanoparticles in Analytical and Medical Devices. *Elsevier*. DOI:https://doi.org/10.1016/B978-0-12-821163-2.00001-7

Holzwarth, U., & Gibson, N. (2011). The Scherrer equation versus the'Debye-Scherrer equation'. *Nature nanotechnology*, 6(9), 534–534. DOI:https://doi.org/10.1038/nnano.2011.145

Ismail, A. M., Menazea, A., Kabary, H. A., El-Sherbiny, A., & Samy, A. (2019). The influence of calcination temperature on structural and antimicrobial characteristics of zinc oxide nanoparticles synthesized by Sol–Gel method. *Journal of Molecular Structure*, 1196, 332–337. DOI:https://doi.org/10.1016/j.molstruc.2019.06.084

Ismail, S. M., & Ahmed, S. M. (2023). The effect of calcination temperatures on the properties of ZnO nanoparticles synthesized by using leaves extracts of pinus brutia tree. *Science Journal of University of Zakho*, 11(2), 286–297. DOI:https://doi.org/10.25271/sjuoz.2023.11.2.1087

Kaur, A., Kaur, H., Singh, R., & Singh, V. K. (2025). Implications on Structural, Morphological, and Optical Properties and Photocatalytic Degradation Behavior of Zinc Oxide Nanoparticles: Effect of Calcination Temperature. *JOM*, 1–11. DOI:https://doi.org/10.1007/s11837-025-07344-9

Kayaci, F., Vempati, S., Donmez, I., Biyikli, N., & Uyar, T. (2014). Role of zinc interstitials and oxygen vacancies of ZnO in photocatalysis: A bottom-up approach to control defect density. *Nanoscale*, 6. DOI:http://dx.doi.org/10.1039/c4nr01887g

Khan, S., & Hossain, M. K. (2022). Classification and properties of nanoparticles. *Nanoparticle-based polymer composites*, 15–54. DOI:https://doi.org/10.1016/B978-0-12-824272-8.00009-9

Kotousov, A., Khanna, A., & Bun, S. (2014). An analysis of elasto-plastic fracture criteria. *Recent Advances in Structural Integrity*

*Analysis - Proceedings of the International Congress (APCF/SIF-2014)*, 67–71. DOI:https://doi.org/10.1533/9780081002254.67

Kumar, S., Hussain, A., Siddiqui, A. M., Khan, Z. H., Abdullah, M. M., & Ashraf, M. T. (2024). Synthesis and study of the impact of calcination duration on the properties of Al4 (ZnO) 96 nanoparticles. *Nano-Structures and Nano-Objects*, 39, 101250. DOI:https://doi.org/10.1016/j.nanoso.2024.101250

Loza, K., Epple, M., & Maskos, M. (2019). Stability of nanoparticle dispersions and particle agglomeration. *Biological Responses to Nanoscale Particles: MolecularCellular Aspects Methodological Approaches*, 85–100. DOI:https://doi.org/10.1007/978-3-030-12461-8_4

Mahajan, M., Kumar, S., Gaur, J., Kaushal, S., Dalal, J., Singh, G., ..., & Ahlawat, D. S. (2025). Green synthesis of ZnO nanoparticles using Justicia adhatoda for photocatalytic degradation of malachite green and reduction of 4-nitrophenol. *RSC advances*, 15(4), 2958–2980. DOI:https://doi.org/10.1039/D4RA08632E

Mahato, S. S., Mahata, D., Panda, S., & Mahata, S. (2023). Perspective chapter: sol-gel science and technology in context of nanomaterials–recent advances. *Sol-Gel Method-Recent Advances*. DOI:https://doi.org/10.5772/intechopen.111378

Malik, S., Muhammad, K., & Waheed, Y. (2023). Nanotechnology: a revolution in modern industry. *Molecules*, 28(2), 661. DOI:https://doi.org/10.3390/molecules28020661

Mohamed, A. F., & Mawlud, S. Q. (2023). Effect of zinc oxide on structural and optical properties borotellurite glass: ternary glass. *Zanco Journal of Pure Applied Sciences*, 35(4), 14–21. DOI:http://dx.doi.org/10.21271/ZJPAS.35.4.02

Nagar, V., Singh, T., Tiwari, Y., Aseri, V., Pandit, P. P., Chopade, R. L., ..., & Awasthi, G. (2022). ZnO Nanoparticles: Exposure, toxicity mechanism and assessment. *Materials Today: Proceedings*, 69, 56–63. DOI:https://doi.org/10.1016/j.matpr.2022.09.001

Nandhini, J., Karthikeyan, E., & Rajeshkumar, S. (2024). Green synthesis of zinc oxide nanoparticles: eco-friendly advancements for biomedical marvels. *Resources Chemicals and Materials*. DOI:https://doi.org/10.1016/j.recm.2024.05.001

Onugwu, A. L., Nwagwu, C. S., Onugwu, O. S., Echezona, A. C., Agbo, C. P., Ihim, S. A., ..., & Khutoryanskiy, V. V. (2023). Nanotechnology based drug delivery systems for the treatment of anterior segment eye diseases. *Journal of Controlled Release*, 354, 465–488. DOI:https://doi.org/10.1016/j.jconrel.2023.01.018

Owuna, F. J. (2020). Stability of vegetable based oils used in the formulation of ecofriendly lubricants – a review. *Egyptian Journal of Petroleum*, 29(3), 251–256. DOI:https://doi.org/10.1016/j.ejpe.2020.09.003

Pal Singh, R. P., Hudiara, I. S., & Bhushan Rana, S. (2016). Effect of calcination temperature on the structural, optical and magnetic properties of pure and Fe-doped ZnO nanoparticles. *Materials Science-Poland*, 34(2), 451–459. DOI:https://doi.org/10.1515/msp-2016-0059

Parajuli, D., Dangi, S., Sharma, B. R., Shah, N. L., & KC, D. (2023). Sol-gel synthesis, characterization of ZnO thin films on different substrates, and bandgap calculation by the Tauc plot method. *Bibechana*, 20(2), 113–125. DOI:https://doi.org/10.3126/bibechana.v20i2.54115

Roy, A., Healey, C. P., Larm, N. E., Ishtaweera, P., Roca, M., & Baker, G. A. (2024). The huge role of tiny impurities in nanoscale synthesis. *ACS Nanoscience Au*, 4(3), 176–193. DOI:https://doi.org/10.1021/acsnanoscienceau.3c00056

Sa, Y., Guo, Y., Feng, X., Wang, M., Li, P., Gao, Y., ..., & Jiang, T. (2017). Are different crystallinity-index-calculating methods of hydroxyapatite efficient and consistent? *New Journal of Chemistry*, 41(13), 5723–5731. DOI:https://doi.org/10.1039/C7NJ00803A

Samantaray, S., Mallick, P., Hung, I.-M., Moniruzzaman, M., Satpathy, S. K., & Mohanty, D. (2024). Ceramic-ceramic nanocomposite materials for energy storage applications: A review. *Journal of Energy Storage*, 99, 113330. DOI:https://doi.org/10.1016/j.est.2024.113330

Shafiee, P., Nafchi, M. R., Eskandarinezhad, S., Mahmoudi, S., & Ahmadi, E. (2021). Sol-gel zinc oxide nanoparticles: advances in synthesis and applications. *Synthesis Sintering*, 1(4), 242–254. DOI:https://doi.org/10.53063/synsint.2021.1477

Sharma, R., Sharma, A., Chuhadiya, S., Thakur, A., Kannan, M., & Dhaka, M. (2023). Air annealing evolution to physical characteristics of Cd0. 85Zn0. 15Te thin films: absorber layer applications to solar cell devices. *Journal of Materials Science: Materials in Electronics*, 34(18), 1403. DOI:https://doi.org/10.1007/s10854-023-10759-2

Sharma, V., Sharma, J., Kansay, V., Sharma, V. D., Sharma, A., Kumar, S., ..., & Bera, M. (2023). The effect of calcination temperatures on the structural and optical properties of zinc oxide nanoparticles and their influence on the photocatalytic degradation of leather dye. *Chemical Physics Impact*, 6, 100196. DOI:https://doi.org/10.1016/j.chphi.2023.100196

Şimşek, T., Ceylan, A., Aşkın, G. Ş., & Özcan, Ş. (2022). Band gap engineering of ZnO nanocrystallites prepared via ball-milling. *Politeknik Dergisi*, 25(1), 89–94. DOI:https://doi.org/10.2339/politeknik.647702

Sridar, R., Ramanane, U. U., & Rajasimman, M. (2018). ZnO nanoparticles – Synthesis, characterization and its application for phenol removal from synthetic and pharmaceutical industry wastewater. *Environmental Nanotechnology, Monitoring & Management*, 10, 388–393. DOI:https://doi.org/10.1016/j.enmm.2018.09.003

Sugihartono, I., Retnoningtyas, A., Rustana, C., Umiatin, Yudasari, N., Isnaeni, ..., & Kurniadewi, F. (2019). The influence of calcination temperature on optical properties of ZnO nanoparticles. *AIP Conference Proceedings*.

Supin, K. K., PM, P. N., & Vasundhara, M. (2023). Enhanced photocatalytic activity in ZnO nanoparticles developed using novel Lepidagathis ananthapuramensis leaf extract. *RSC advances*, 13(3), 1497–1515. DOI:https://doi.org/10.1039/D2RA06967A

Tripathy, N., & Kim, D.-H. (2018). Metal oxide modified ZnO nanomaterials for biosensor applications. *Nano convergence*, 5(1), 27. DOI:https://doi.org/10.1186/s40580-018-0159-9

Usman, A., Aris, A., Labaran, B., Darwish, M., & Jagaba, A. (2022). Effect of calcination temperature on the morphology, crystallinity, and photocatalytic activity of ZnO/TiO2 in selenite photoreduction from aqueous phase. *J. New Mater. Electrochem. Syst.*, 25(4), 251–258. DOI:https://doi.org/10.14447/jnmes.v25i4.a05

Zubair, M. A., Mouri, T. K., & Chowdhury, M. T. (2023). Influence of Cu induced crystallographic disorder on the optical and lattice vibrational properties of ZnO nanoparticles. *Physical Chemistry and Chemical Physics*, 25(40), 27628–27653. DOI:https://doi.org/10.1039/D3CP02015K